Supplement of Geochronology, 6, 697–717, 2024
https://doi.org/10.5194/gchron-6-697-2024-supplement
© Author(s) 2024. CC BY 4.0 License.

Supplement of

Interpreting cooling dates and histories from laser ablation in situ (U–Th–Sm) / He thermochronometry: a modelling perspective

Christoph Glotzbach and Todd A. Ehlers

Correspondence to: Christoph Glotzbach (christoph.glotzbach@uni-tuebingen.de)

The copyright of individual parts of the supplement might differ from the article licence.

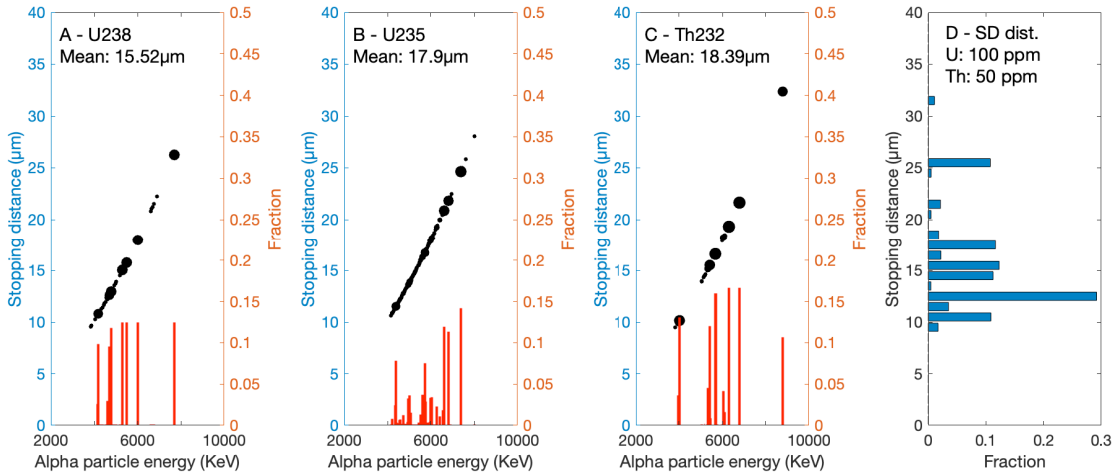

Fig. S1: Alpha particle energy spectra of ^{238}U (A), ^{235}U (B), and ^{232}Th (C) and corresponding stopping distance spectra and mean stopping distances derived from SRIM2013 data assuming a zircon with a density of 4.65 g/cm^3 and radionuclide concentrations of 100 ppm U and 50 ppm Th (D).

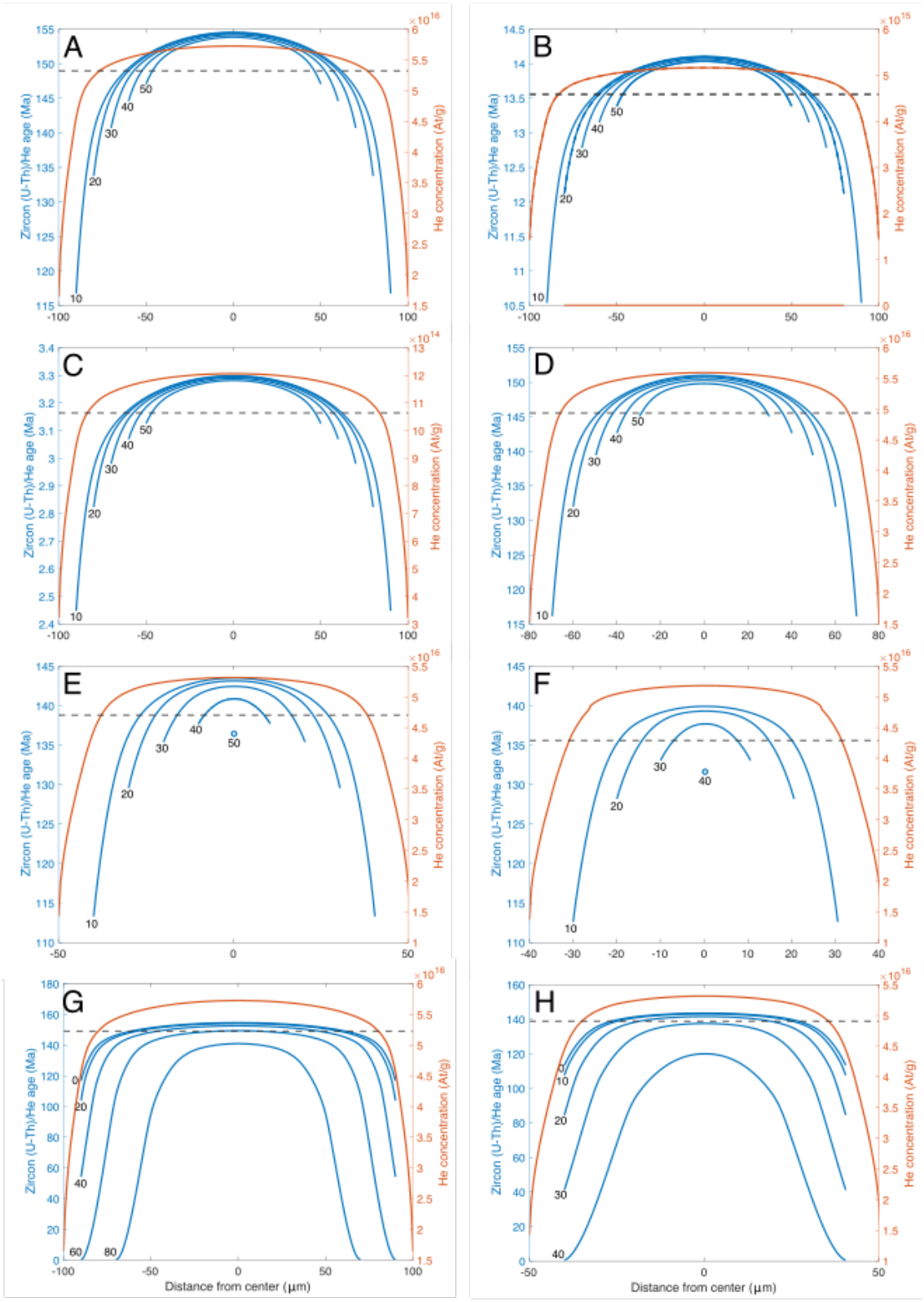

Fig. S2: Predicted in-situ zircon (U-Th)/He dates (blue lines) and He concentration profile (orange line) for an infinitely long, cylindrical-shaped zircon with homogenous radiogenic nuclide distribution (U and Th concentration of 100 and 50 ppm, respectively). Predicted dates are calculated by integrating modeled He distribution over an entire ablation pit volume of variable diameters (black numbers on curves in A-D) that is continuously measured across the grain. In reality, discrete (rather than continuous) pits would be measured and smooth curves such as those shown here would not be possible to measure. A) Model

results assuming a constant cooling of 10°C/Myr to a final temperature of 10°C and a grain radius of 100 µm. The corresponding whole grain date for a sphere with a similar sphere equivalent radius (radius*1.5) corrected for alpha ejection is 6.5 Ma. Modeled in-situ dates with variable spot diameters (10, 20, 30, 40 and 50 µm) range from 8.3 Ma in the center of the grain to 4.9 Ma, half the spot diameter away from the grain rim. B) Model results assuming constant cooling with 1°C/Myr to 0°C and a grain radius of 100 µm. The corresponding whole grain date corrected for alpha ejection is 49.7 Ma. Modeled in-situ dates with variable spot diameters (10-50 µm) range from 64.9 Ma in the center of the grain to below 37.7 Ma, half the spot diameter away from the grain rim. C,D) Same as B) but with a grain radius of 80 and 50 µm. The smaller grain radius results in lower whole-grain dates (46.9 and 41.8 Ma) and stronger relationship between in-situ dates and distance of measurement towards the grain rim. E) In-situ dates for a grain radius of 100 µm and spot diameter of 10 µm. Dates have been calculated for the central plane, dividing the cylinder in two symmetrical sides along the crystallographic c-axis (black number 0 - 0 µm in r-direction of Fig. 2 in the manuscript) and at other r-planes 20, 40, 60 and 80 µm. F) In-situ dates for a grain radius of 50 µm and spot diameter of 10 µm. Dates have been calculated for the central plane and at other r-planes 10, 20, 30, 40 µm.

S1: Quantification of radionuclide variations

Here we have used LA-ICP-MS measurements to quantify radionuclide zoning by measuring U and Th against Ca (apatite) and Zr (zircon) with depth. Measurements have been taken in the center of previously polished grains to depth of 30-60 µm. Downhole fractionation correction was applied using NIST610/612 calibration standards and 43Ca (apatite) and 29Si (zircon) as internal standard. A set of randomly selected samples have been measured, including apatite age standards (Durango and McClure), zircon age standards (91500, Fish Canyon and Plesovice), and samples from South American granitoids (LCTE…, SGTE… and 18PG55), upper Triassic sandstone from Germany (Schoen2), Paleogene sediments from the Pyrenees (CLA4-SER4) and present-day sediments from alpine rivers (DK2005 and DK2009a,b).
Time-resolved LA-ICP-MS measurements of U/Ca and Th/Ca in 421 apatites and U/Zr and Th/Zr in 383 zircons do show a large range of possible U and Th distribution patterns (Fig. S3). Analyzed age standards do show no (Durango, 91500, Plesovice), slight (McClure) to significant (Fish Canyon) zoning (Fig. S3A,B). Most apatite and especially zircon samples show variations in radionuclides with depth (Fig. S3I-P). In most cases, U and Th are positively correlated and show either an increase (Fig. S3C,D,K,L) or a decrease (Fig. S3E,F,M,N) from core to rim. More complex patterns with several peaks are very common (Fig. S3G,H,I,J) and a few grains do show an anti-correlation between U and Th (Fig. S3O,P).

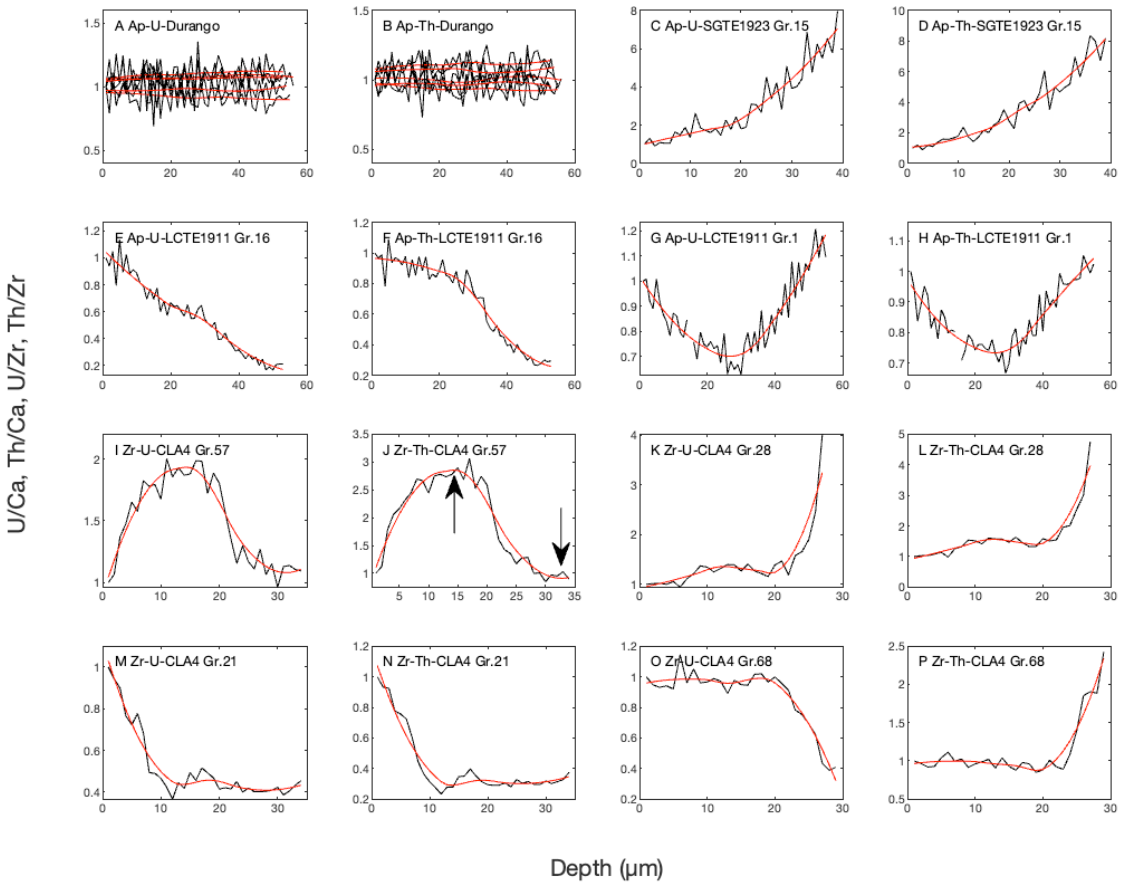

Fig. S3: Radionuclide (U and Th) variations within selected apatite (A-H) and zircon (I-P) grains. U/Ca and Th/Ca ratios are shown for apatites and U/Zr and Th/Zr ratios for zircons. The original data (black line) and a smoothed fit (red line) are shown. From the latter, we derived the extreme values and positions, as shown in J.

We derived the most extreme deviation from uniform U and Th concentrations ($R_{max/min}$) for all analyzed apatite and zircons grains using the following equation:

$$R_{max/min} = \frac{\max R_i}{\min R_i} \qquad \text{Eq. S1}$$

Where R_i is radionuclide to stochiometric element ratio (e.g. U/Ca or U/Zr) normalized to the core R_i. Nearly half the apatite grains show an enrichment of U and/or Th in the rim relative to the core, whereas the other half show a depletion (Fig. S4). Uranium in apatite does show the weakest zoning with an average rim-to-core ratio of 1.09±0.51. Thorium in apatite is behaving similarly, but the higher standard deviation (1.53 vs. 0.51 in Ap-U) does reflect overall higher variation with both rim-enriched and -depleted grains. Those grains with depleted rims (47%) have an average U ratio of 0.81±0.17 only 5% of those grains have a ratio <0.5 (Fig. S4). Similarly, only 5% show 2 times or more increased U concentration in the rim relative to the core. The corresponding mean rim-to-core U ratio is 1.33±0.57. The behavior of Th is quite similar since U and Th are mostly correlated.
The majority of analyzed zircons show enriched rims, 60% of grains are enriched in Th and 64% in U. As a result, the average rim-to-core radionuclide ratio is 1.51 (U) and 1.58 (Th), significantly higher compared to apatite (Fig. S4). Only 36% of zircons have a depleted rim-to-core U ratio with a mean of 0.71±0.21, and only 6% have ratios <0.5. Those grains with enriched rim-to-core U ratio mean values of 1.95±2.06, and 17% do have >2 times enriched core-to-rim ratios.

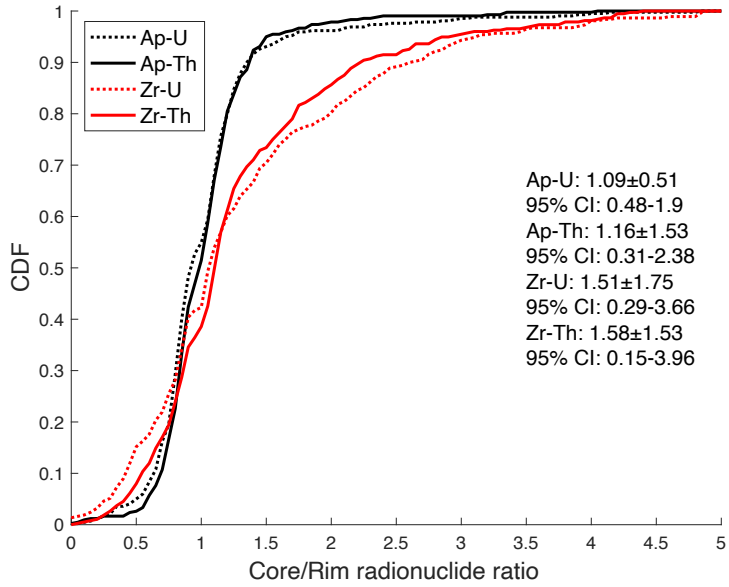

Fig. S4: Most extreme core-to-rim ratio of U and Th of analyzed apatite and zircon grains. Calculated mean values with standard deviations for the different minerals and radionuclides range between 1.09 (nearly as many grains have enriched or depleted rims) to 1.58 (more grains have enriched rims or show stronger enrichment compared to depleted rims).

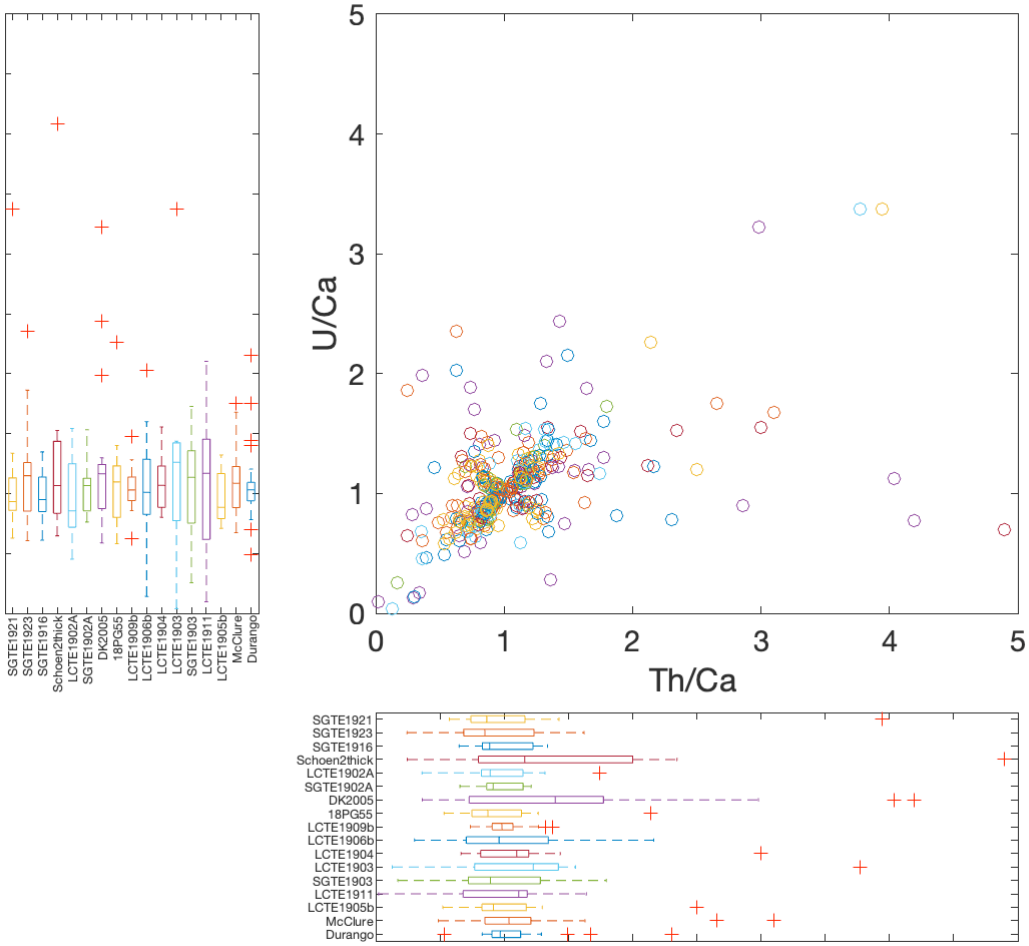

Fig. S5: Compilation of U/Ca and Th/Ca ratios for 421 apatite grains from 17 samples. For each grain the most extreme normalized U/Ca and Th/Ca ratios were extracted and plotted against each other. Values >1 correspond to an increase in the U/Ca or Th/Ca ratio along the analyzed grain profile, whereas values <1 imply a decrease in ratios. The absence of radionuclide zoning would result in a value of 1. Statistics of each sample are shown as boxplots with median (central line), 25th and 75th percentile (box), maximum and minimum value (hatched line), and outliers red crosses.

S2: Effect of radionuclide zoning on whole grain (U-Th-Sm)/He ages

In-homogenous distribution of radionuclides and the long-alpha stopping distance of He do result in a complex distribution of He in mineral grains. Ft-correction factors required for whole grain (U-Th-Sm)/He analyses would be largely different for grains with spatial variations in radionuclide concentrations (e.g. Hourigan et al. 2005). Radionuclide depletion and enrichment of grain rims can lead to Ft-correction factors deviating from the 'assumed' Ft-correction factor calculated with uniform radionuclide distribution by up to 40% (Hourigan et al. 2005).
Here we have calculated theoretical single-grain ages for apatite grains with radionuclide zoning, assuming that they are not zoned. Single grain ages vary between ~33 to ~84 Ma for a grain radius of 100 µm and a rim radius between 1 to 99 µm, a ratio between radionuclide concentrations between the core and rim between 0.05 to 20, cooling rate of 1°C/Myr and grain averaged U, Th and Sm concentrations of 10 ppm. For a cooling rate of 10°C/Myr and similar parameters, whole grain ages vary between ~4.4 to ~8.6 Ma. Allowing the mean radionuclide concentrations to vary as well would increase the spread in ages even more, e.g. for eU values above 100 ppm, ages can be as old as 100 Ma and 10 Ma for cooling rates of 1°C/Myr and 10°C/Myr, respectively.
Obviously, the thickness and position of the enriched/depleted zone within a grain are important for the deviation in whole grain ages. Enriched thin rims (<30 µm) and depleted cores (<80 µm) result in the largest deviation.
The position of measured extrema in the U and Th distribution of analyzed apatite and zircon grains vary (Fig. S6), whereas ~40% (zircon) and ~30% (apatite) do have enriched rims with an average core/rim ratio of ~0.5 (Fig. S6). Enriched cores are less common (~20% of zircons and ~25% of apatites), and average core/rim ratios are ~1.5. Such core/rim ratios do lead to age deviations around 5-10% (Fig. S6), assuming a simple step distribution of radionuclides.

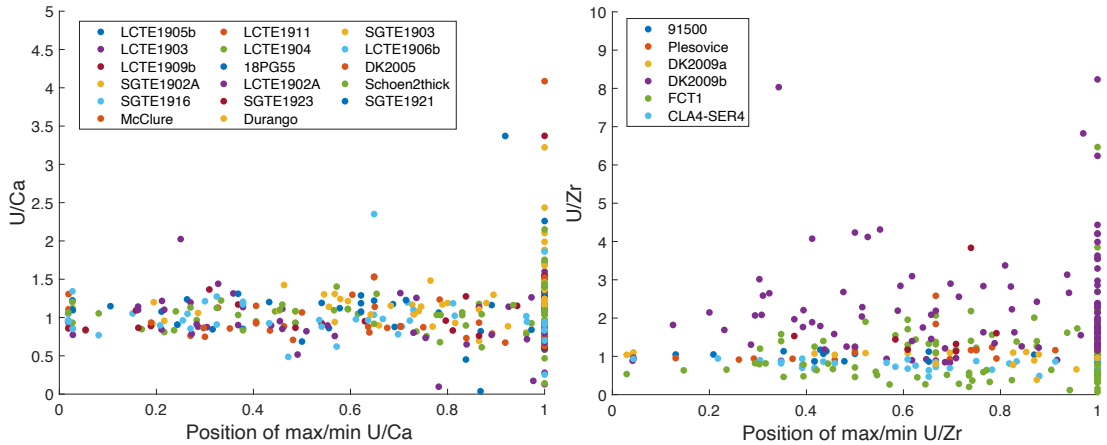

Fig. S6: Absolute extrema of U/Ca and U/Zr ratios plotted against the position at which this extremum is occurring. A position of 0 means in the center of the grain, and a value of 1 correspond to the outermost part measured (roughly 30 microns away from the core).

More realistic estimates on the effect of the observed radionuclide distribution on (U-Th-Sm)/He ages do require the incorporation of measured U and Th concentration profiles. We have scaled observed variations to a common grain radius of 100 µm and calculated apatite and zircon (U-Th-Sm)/He ages. Single grain apatite ages vary between 51 and 83 Ma, while the mean ages of samples vary from 53 Ma (18PG55) to 78 Ma (Mad) and are a function of the mean eU of individual grains. A similar but less pronounced trend is visible in ZHe ages that vary from 117 to 178 Ma, and individual samples have mean ages of 148 to 162 Ma. The lower intra-sample variability of ZHe ages is likely an artifact of the difference in sample size. Assuming that observed variations in eU and zoning of radionuclides in our apatites and zircons are representative, we can expect overdispersion of AHe and ZHe ages.
In addition, we calculated corresponding ages without radionuclide variations using grain-specific averaged U, Th, and Sm concentrations (Fig. S7). For a constant cooling rate of 1°C/Myr, apatite ages (taking into account zoning) mostly depend on eU (R^2=0.95) (Fig. S7A). The remaining 5% of the variability is the result of radionuclide zoning. Modeled ZHe ages do reveal a larger spread in ages, whereas 23% of the variability in the data is caused by radionuclide zoning (Fig. S7B). Individual samples usually do not show that large spread in eU and correspondingly, the zoning-induced variability can be expected to be larger, especially for those samples with relatively similar eU concentrations but variable zoning. The variability in apatite ages caused by zoning in individual samples ranges from 1% (LCTE1905b) to 40% (SGTE1921), with a mean of all analyzed samples of 13%. On average, 52% of the variability in ZHe ages is caused by radionuclide zoning in individual samples (Fig S7B). In samples with a low spread in eU and strong radionuclide zoning, the majority of variability is caused by zoning, and there is no significant relation with eU, e.g. in Fish Canyon tuff 84% of the age spread is due to zoning (Fig. S7B).

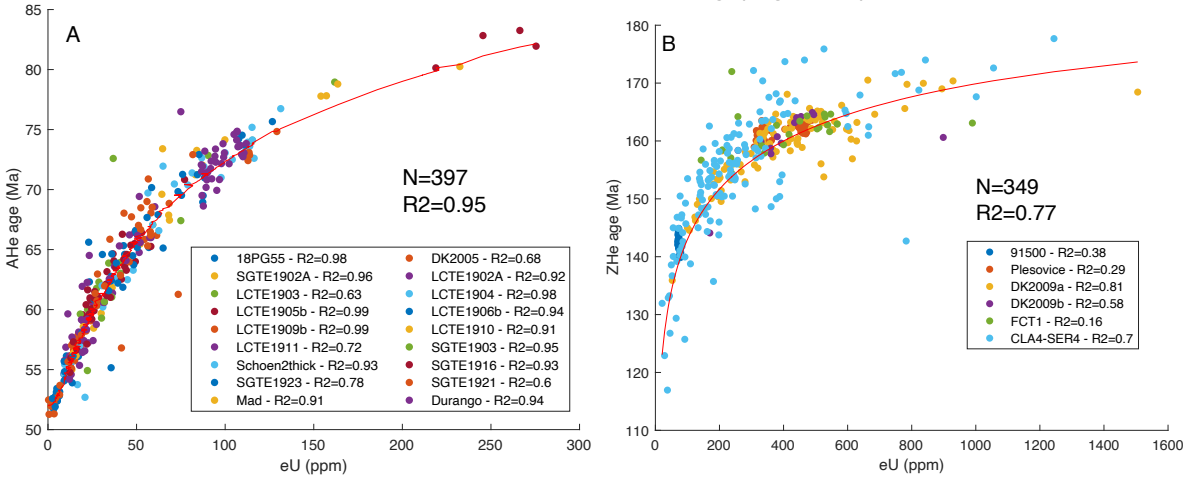

Fig. S7: Modelled apatite (A) and zircon (B) (U-Th-Sm)/He ages for a constant cooling of 1°C/Ma, a grain radius of 100 µm, and grain-specific U, Th, and Sm concentration profiles. Assuming homogenous radionuclide distributions result in ages following the red line.

S3: How many grains are needed for whole-grain (U-Th-Sm)/He analysis

Here we used several hundred LA-ICP-MS measurements made in our lab at the University of Tuebingen. Most of our samples are characterized by ~20 grains, but typical whole grain analyses do measure 3-5 grains, increasing the likelihood of high variability in ages not correlating with eU. We tested this hypothesis and determined the optimal sample size using a Monte Carlo approach. Theoretical samples with 3 to 30 individual grains were randomly

collected from all analyzed grains. The coefficient of determination (R^2) between the randomly picked set of grains and the correct relation between age vs. eU (red line in Fig. S7) was calculated 20000 times. The mean R^2 and the confidence interval at 2σ show slightly different dependence on the number of grains for whole-grain analyses for apatite and zircon (U-Th-Sm)/He data (Fig. S8). Less pronounced radionuclide zoning of apatite compared to zircon does result in overall higher R^2, and the spread in the data is strongly decreasing from 3 to 8 grains. A similar rapid decrease in R^2 with increasing sample size is not obvious in the modeled ZHe data. Based on the measured radionuclide zoning and the modeling approach, we can suggest that a minimum of 10 whole-grain AHe ages are needed to reach a minimum R^2 of 0.8 (at 2σ). An unrealistic 23 whole-grain ZHe ages are theoretically needed to reach a minimum R^2 of 0.5 (at 2σ).

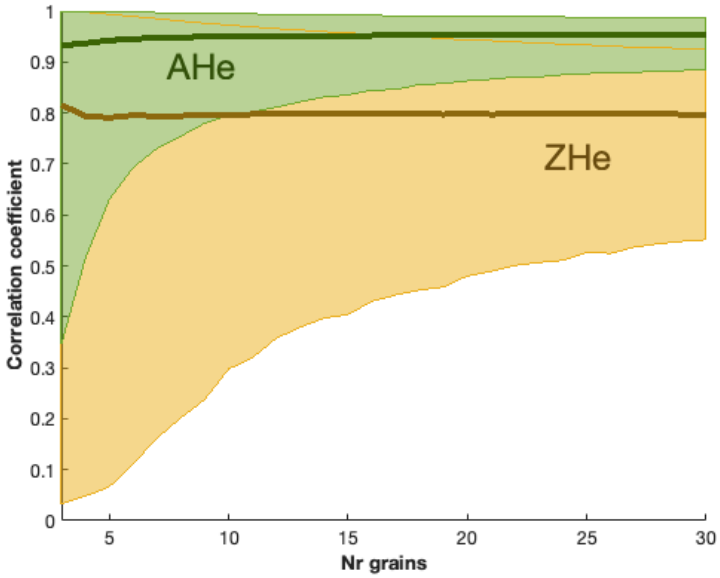

Fig. S8: Results of a Monte Carlo approach to determine the dependency of the number of whole grain analyses and expected correlation to the correct eU vs. age relation. The correlation coefficient is determined between (U-Th-Sm)/He ages with measured zoning and (U-Th-Sm)/He ages assuming homogeneous radionuclide distribution (the red-line in Fig. S7).

S4: In-situ (U-Th-Sm)/He dates of inversion experiments

Synthetic inversions based on in-situ (U-Th-Sm)/He data of two grains with grain radius of 40 and 80 µm were performed. The reconstructed tT-path is shown in Fig. 11 of the manuscript, while the corresponding He profiles and dates are shown here (Fig. S9).

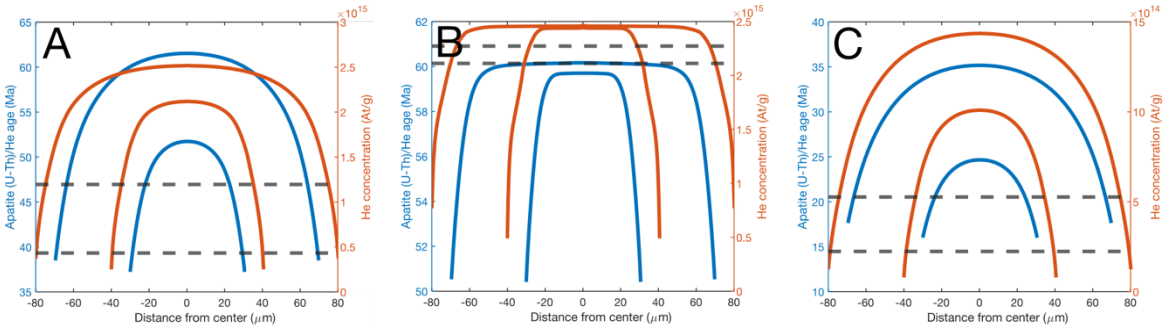

Fig. S9: Predicted in-situ apatite (U-Th-Sm)/He dates (blue lines) and He concentration profile (orange line) for an infinitely long, cylindrical-shaped apatite with homogenous radiogenic nuclide distribution (U, Th and SM concentration of 10 ppm, respectively) and grain radius of 80 and 40 µm. Predicted dates are calculated by integrating modeled He distribution over an entire ablation pit volume of 20 µm diameter that is continuously measured across the grain. A) Data was calculated with a constant cooling rate of 1°C/Myr. B) Input data were modelled with rapid cooling at 60 Ma to surface temperature. C) Initial slow cooling with 1°C/Myr to 50°C at 10 Ma is followed by faster cooling to the surface with 4°C/Myr.